RESEARCH

Backscatter from therapeutic doses of ionizing irradiation does not impair cell migration on titanium implants in vitro

Lisa Printzell[1] · Janne Elin Reseland[2] · Nina Frederike Jeppesen Edin[3] · Jan Eirik Ellingsen[1] · Hanna Tiainen[2]

Abstract

Objective The influence of radiation backscatter from titanium on DNA damage and migration capacity of human osteoblasts (OBs) and mesenchymal stem cells (MSCs) may be critical for the osseointegration of dental implants placed prior to radiotherapy. In order to evaluate effects of radiation backscatter, the immediate DNA damage and migration capacity of OBs and MSCs cultured on titanium or plastic were compared after exposure to ionizing irradiation.

Materials and methods Human OBs and MSCs were seeded on machined titanium, moderately rough fluoride-modified titanium, or tissue culture polystyrene, and irradiated with nominal doses of 2, 6, 10, or 14 Gy. Comet assay was performed immediately after irradiation, while a scratch wound healing assay was initiated 24 h post-irradiation. Fluorescent live cell imaging documented the migration.

Results DNA damage increased with higher dose and with backscatter from titanium, and MSCs were significantly more affected than OBs. All doses of radiation accelerated the cell migration on plastic, while only the highest dose of 10 Gy inhibited the migration of both cell types on titanium.

Conclusions High doses (10 Gy) of radiation inhibited the migration capacity of both cell types on titanium, whereas lower doses (2 and 6 Gy) did not affect the migration of either OBs or MSCs.

Clinical relevance Fractionated doses of 2 Gy/day, as distributed in conventional radiotherapy, appear not to cause severe DNA damage or disturb the migration of OBs or MSCs during osseointegration of dental implants.

Keywords Radiation backscatter · Titanium implants · DNA damage · Cell migration · Mesenchymal stem cells · Osteoblasts

Introduction

Oral sequelae of radiotherapy (RT) are mutilating to head and neck cancer patients [1]. Preradiotherapy dental extractions are necessary for most of these patients [2], which may affect their appearance, impair their ability to speak and chew, and have an overall negative impact on the patients'

health-related quality of life [3, 4]. Temporary removable dentures are experienced as painful and they do not fulfill their desired functional purpose during the first 6 months after RT [5]. Compared to conventional complete- or partial-dentures, implant retained prostheses are recognized to be superior regarding masticatory performance, patients' satisfaction, and quality of life [6, 7]. Despite the impaired healing capacity of irradiated bone, these major benefits make dental implants a feasible and valued treatment for many patients undergoing RT [8–11]. Thus, early permanent prosthetic reconstructions should be prioritized to help restore oral function to an acceptable level for the well-being of head and neck cancer patients [12].

Clinicians are increasingly recognizing the benefits of installing implants in head and neck cancer patients immediately after removal of teeth, prior to RT (primary placement) [13, 14], rather than the traditional delayed installation

✉ Lisa Printzell
lisa.printzell@odont.uio.no

1 Department of Prosthodontics, Institute of Clinical Dentistry, Faculty for Dentistry, University of Oslo, PO box 1109, 0317 Blindern, Oslo, Norway

2 Department of Biomaterials, Institute of Clinical Dentistry, Faculty for Dentistry, University of Oslo, Oslo, Norway

3 Department of Physics, Faculty of Mathematics and Natural Science, University of Oslo, Oslo, Norway

🖄 Springer

during the post-treatment follow-up (secondary placement) [15] which postpones the oral rehabilitation for years. In addition to providing these patients with functional prosthetic reconstructions as early as possible, survival rates of primary placed dental implants are comparable to those with secondary placement [13, 16]. Nevertheless, oral rehabilitation of head and neck cancer patients with the use of dental implants lacks consensus and recommendations regarding the timing of the surgery.

One central clinical concern towards primary placement of dental implants has been the effects of radiation backscatter from titanium, resulting in a higher dose of radiation to the tissues surrounding the implant [17, 18]. In the absence of conclusive clinical evidence, the question whether radiation backscatter impairs the osseointegration process of implants placed prior to RT to a larger extend than the reduced healing capacity of previously irradiated bone in the case of secondary placement still persists. Therefore, more studies are needed to identify the cellular effects of radiation backscatter, and thereby, proceed towards validation of primary placement of dental implants in patients planned for RT.

Ionizing radiation may cause either direct disruption of atomic structures in DNA molecules or indirectly affect it by cleavage of water molecules that form free water radicals, which in turn may ionize DNA [19]. Radiation-induced DNA damage activates cell responses depending on the severity of the lesion: either an apoptotic signalling cascade eliminates the cell or the cell will stop dividing while DNA repair enzymes try to repair the damage [20–22]. The goal of RT is always to maximize the genotoxic effect in the tumor, while limiting radiation injury to surrounding normal tissues [19]. In conventional RT, this is achieved by distributing the radiation in dose fractions, typically 2 Gy per day over 5–7 weeks [23].

The osseointegration of a titanium implant is a process similar to wound healing [24, 25]. Since cell migration is a rate-limiting event in wound healing, in vitro analysis of this ability is important in order to evaluate the osseointegration potential. Interestingly, low-level laser irradiation has shown to stimulate a range of cellular processes and promote soft and hard tissue repair in rats [26, 27]. However, no study has yet investigated the effects of *therapeutic* doses of ionizing irradiation on the migration of cells involved in the osseointegration process. In this study, primary human OBs and MSCs were exposed to clinically relevant doses of γ-radiation to assess the biological effects caused by the radiation reinforced with backscatter from titanium implant surfaces. For this purpose, radiation-induced single and double-strand DNA damage was determined by the comet assay and the cell migration capacity was evaluated in a wound healing scratch assay.

Material and methods

Test surfaces

Commercially pure (cp) minimally rough grade 2 titanium (Ti) and moderately rough fluoride-modified grade 4 titanium (TiF) disks with a diameter of 6.25 mm and height of 1.95 mm were used as test surfaces, with tissue culture polystyrene (TCP) serving as a control surface for assessing the effect of radiation backscatter. The machined Ti-surfaces were washed first in trichloroethylene for 15 min, then in absolute ethanol (100%) in an ultrasonic bath for 15 min, before being sterilized in an autoclave at 135 °C for 20 min. The TiF-surfaces were manufactured by Dentsply Sirona implants according to the same protocol as the commercially available implant surface Osseospeed. The disk surface was grit-blasted with titanium dioxide (TiO_2) microparticles, followed by an initial etching in concentrated nitric acid (HNO_3) and sodium hydroxide (NaOH), respectively, and a final etching step in 0.1 M hydrofluoric acid (HF) before being pre-mounted on carriers in sealed containers and sterilized by β-irradiation (Osseospeed, Dentsply Sirona implants, Mölndal, Sweden).

Cell culture

Commercially available primary human osteoblasts (OBs; batch#: 0000426160) and human mesenchymal stem cells (MSCs; batch#: 0000684888) (Lonza, Walkersville, MD, USA) were routinely cultured at 37 °C/5% CO_2 in osteoblast basal medium (C-27010) supplemented with Osteoblast Growth Medium SupplementMix (C-39615) (Promocell, Heidelberg, Germany), or in human Mesenchymal Stem Cell Growth BulletKit Medium (MSCGM catalog no. PT-3001) (Lonza) respectively, both containing L-glutamine, gentamicin sulfate-amphotericin (GA), and 10% fetal bovine serum (FBS). Cells were subcultured before reaching confluence using trypsin/EDTA (Sigma-Aldrich). Trypan blue staining was used to determine total and viable cell number. Cells were seeded at a density of 3.5×10^3 cells/well on TCP and 4.5×10^3 cells/disk on Ti and TiF disks in 96-well plates for the comet assay, and at a density of 7.5×10^4 cells/well or disk in 48-well plates for the wound healing assay and incubated overnight at 37 °C/5% CO_2 prior to irradiation. Experiments were performed with cells at passages < 7 after isolation.

Following overnight incubation, the basal growth medium was changed and the cells on the different sample surfaces were exposed to various doses of γ-radiation. Irradiation times for nominal doses of 2, 6, 10, and 14 Gy were calculated considering the source-to-plate distance of 70 cm and the decay of the ^{60}Co source (Theratron 780-C, MDS

Nordion, Ontario, Canada). A dose of 10 Gy delivered on a titanium surface is equivalent to a dose of 14 Gy delivered on TCP, taking the additional radiation backscatter into account [28]. Therefore, the highest dose of 14 Gy was only used for cells cultured on TCP. To maintain the cell medium temperature at 37 °C, a hollow perspex plate transfused with circulating pre-heated water (Grant Instruments, Cambridge, England) was used throughout the irradiation procedure. Dose measurements were achieved by thermoluminescence dosimetry (TLD) (TLD-100; Harshaw TLD Bicrom, Solon, OH, USA). The irradiation was performed at The Norwegian Radium Hospital, Oslo University Hospital.

Comet assay

An alkaline single cell electrophoreses comet assay was used to quantify immediate DNA damage in OBs and MSCs exposed to various doses of irradiation on the different sample surfaces. The cells were kept on ice whenever practically possible throughout the entire sample preparation process to minimize immediate rejoining of strand breaks induced by the radiation.

Immediately after the irradiation, the cells were detached from sample disks or wells with trypsin/EDTA and resuspended in 225 µl culture media. After centrifugation (5 min at $200 \times g$), the supernatant was removed and the cell pellet was mixed in 26 µl of 1% (w/v) low melting point agarose. The agarose-cell suspension was divided into two equal drops of 12 µl and placed on an agarose-coated microscope slide. Slides were stored at 4°C for 10 min for complete gelation. A positive control (unirradiated cells on TCP) was placed in a slide holder filled with cold 3% H_2O_2 for 5 min. All slides were then placed in slide holders filled with a cold lysis solution (2.5 M NaCl, 100 mM EDTA, 10 mM Tris–HCl, pH = 10, 1% triton X-100) and stored at 4°C for 1 h. All slides were placed in an alkaline electrophoresis solution (300 mM NaOH, 1 mM EDTA, pH > 13) for 20 min at 4°C for DNA unwinding before electrophoresis was run for 30 min at 25 V and 320 mA at 4°C. Slides were neutralized with cold PBS and d-H_2O for 10 min each and dried overnight at 4°C. After drying, the slides were stored at room temperature. For TCP samples, the comet assay was also performed following 24-h incubation after the irradiation using the same protocol for sample preparation.

Nuclei were stained with 0.1 µg/ml SYBR gold (Invitrogen, Eugene, OR, USA) in darkness at room temperature for 15 min shortly before imaging. Slides were imaged using a fluorescence microscope with 4 × objective (Olympus IX70, Olympus, Tokyo. Japan). At least 50 nuclei per droplet (100 per sample; $n = 3$) were imaged and analyzed using the OpenComet plugin (v1.3) for ImageJ. Results of the comet assay are presented as %DNA in tail [29] and as relative DNA damage representing %DNA in tail normalized

to the unirradiated sample on corresponding surface (C⁻) and the positive TCP control (C⁺; 3% H_2O_2) according to the following equation:

$$\mathrm{Relative\,DNA\,damage}(\%) = \frac{\mathrm{Sample} - \mathrm{C}^-}{\mathrm{C}^+ - \mathrm{C}^-} \times 100$$

Wound healing assay

Scratch assay was performed to evaluate the migration capacity of human OBs and MSCs growing on Ti, TiF, and TCP after being exposed to single doses of ionizing γ-irradiation. Following 24 h of incubation at 37 °C/5% CO_2 after the irradiation, the basal growth medium was changed to a serum reduced medium with only 1% FBS to reduce cell proliferation [30]. Two hours later, the cell monolayers were stained with CellTracker Green CMFDA (Invitrogen, Eugene, OR, USA). Scratches formed like a cross were then scraped on each TCP sample using a 200-µl pipette tip, followed by washing with PBS. The cross enabled identification and imaging of the exact same area at each timepoint throughout the experiment (0 h, 6 h, 12 h, 24 h, 30 h, 48 h, 60 h) using an Olympus IX70 fluorescence microscope with 4 × objective (Olympus, Tokyo, Japan). On Ti and TiF-surfaces, the scratch assay was performed with some modifications. Due to the opacity of the Ti and TiF disks, the adherent cells were stained with CellTracker Green CMFDA and disks monitored in a confocal laser scanning microscope before the irradiation to ensure all included samples were covered with a healthy monolayer of OBs or MSCs. Following 24-h incubation at 37 °C/5% CO_2 after the irradiation, cells were stained with CellTracker Green CMFDA again and monitored before a scratch was scraped in a straight line through the cell monolayer on each included disk using a 200-µl pipette tip while holding the disk in place with a tweezer. The scratch was performed in a Petri dish with preheated medium (1% FBS), and then immediately placed in an incubator attached to an upright Leica SP8 confocal laser-scanning microscope with air objective lens HC APO CS 10 × /0.40 (Leica, Wetzlar, Germany) to acquire the baseline image (0 h). With the format of 1024 × 1024, the whole scratch/diameter of the disk was captured in 3 images, which enabled us to find the same area on each disk at each subsequent timepoint (24 h, 48 h, and 72 h).

Upon completion of the experiment, images from each timepoint were analyzed with respect to the gap width and presented as % of total "gap closure" (GC) as illustrated in Fig. S1 in the online supplementary information. Mean measures of each disk from the different timepoints (24 h, 48 h, 72 h) were normalized to 0 h (baseline). The gap edges (measure points) were defined as the recognition of the leading cells on each side of the gap, with maximum 5

countable cells inside the gap that were not already there at 0 h. Additionally, the "gap area filled with cells" (GFC) was estimated and defined as the % of original gap-area evenly filled with cells, without focus on cell density (Fig. S1, Online Resource). ImageJ software (National Institutes of Health and the Laboratory for Optical and Computational Instrumentation) was used for image processing and analysis [31]. The same operator evaluated all images 3 times, on 3 different days, to insure intra-rater reliability. For illustration purposes, background fluorescence was removed from the presented microscopy images of the TCP-surface using Adobe Photoshop 2020. All qualitative and quantitative image analyses were performed before the images were edited.

Data analysis

The effects of irradiation (2, 6, 10, and 14 Gy) on DNA damage and migration capacity of human OBs and MSCs growing on three different surfaces (TCP, Ti, TiF) were graphically presented using Sigmaplot (V 14.0 for Windows; Systat, Chicago, IL, USA). Data from the comet assay is presented as mean values ± standard error of the mean (SEM; $n = 3$). Differences between groups were assessed using one-way ANOVA followed by pairwise multiple comparison using Holm-Sidak method with significance level set to p-values ≤ 0.05. The data was checked for normality and equal variance using Shapiro–Wilk test and Brown-Forsythe test, respectively. Data from the scratch assay is graphically presented using mean values ± standard deviation (SD).

Results

DNA damage

The relative DNA damage in primary human OBs and MSCs immediately (0 h) after exposure to ionizing irradiation (2, 6, 10 Gy) is presented in Fig. 1. Increasing radiation doses induced increasing amounts of DNA damage in both cell types, but MSCs were significantly more affected by radiation than the OBs after all tested doses ($p < 0.05$), and the highest levels of DNA damage were observed in MSCs irradiated on the titanium surfaces, especially the Ti-surface (Fig. 1).

A significantly increased amount of DNA damage was found in unirradiated MSCs on TiF and to a lesser degree on Ti compared to TCP. A similar, but less pronounced and not statistically significant, trend was observed for unirradiated OBs (Fig. S2, Online Resource). After incubating the cells in 10% FBS for 24 h following the irradiation, no dose-dependent difference in DNA damage was observed in either the OBs or MSCs cultured on TCP (Fig. S3, Online Resource). However, the high DNA in tail values observed for all groups following 24-h incubation, including the unirradiated control group, limits the conclusions that could be drawn based on this result.

Wound healing assay

After irradiation, none of the Ti disks contained a confluent monolayer of MSCs. Consequently, the scratch wound healing assay was performed with OBs on TCP, Ti, and TiF, and with MSCs only on TCP and TiF.

Irradiation with 14 Gy increased the migration rate of both OBs (Figs. 2 and 3) and MSCs (Figs. 4 and 5) cultured on TCP, resulting in a total gap closure (GC) within 24 h.
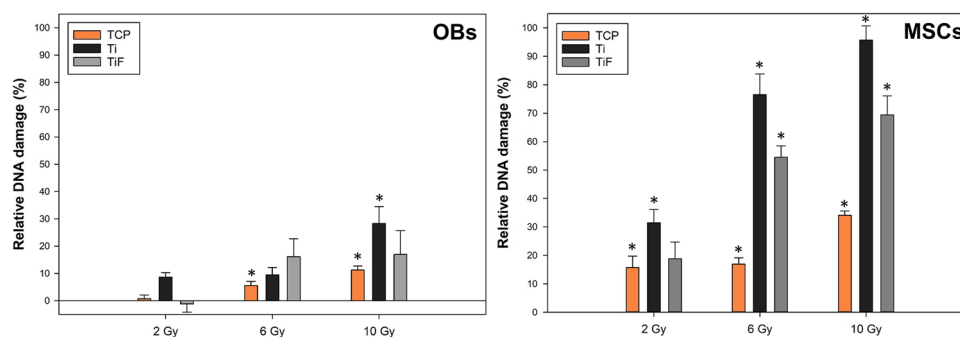

Fig. 1 Relative DNA damage with %DNA in tail normalized to the unirradiated samples on corresponding surface (C⁻) and positive TCP control (C⁺; 3% H$_2$O$_2$), of primary human osteoblasts (OBs) and human mesenchymal stem cells (MSCs) immediately after irradiation with 0, 2, 6, and 10 Gy, while growing on tissue culture polysty-rene (TCP), minimally rough machined titanium (Ti), or moderately rough fluoride-modified titanium (TiF) ($n = 3$). Data are presented as mean ± SEM. * $p \leq 0.05$ compared to corresponding 0 Gy control (C.⁻)

Fig. 2 Representative images of primary human osteoblasts (OBs) migration and gap closure (GC) on tissue culture polystyrene (TCP), minimally rough machined titanium (Ti), and moderately rough fluoride-modified titanium (TiF), after no irradiation and 14 Gy (TCP) or 10 Gy (Ti + TiF), at the timepoints 0, 24, 48, and 72 h. As full gap closure was already observed at 48 h for all TCP samples, no imaging was performed at later timepoints. Scale bar: 200 μm
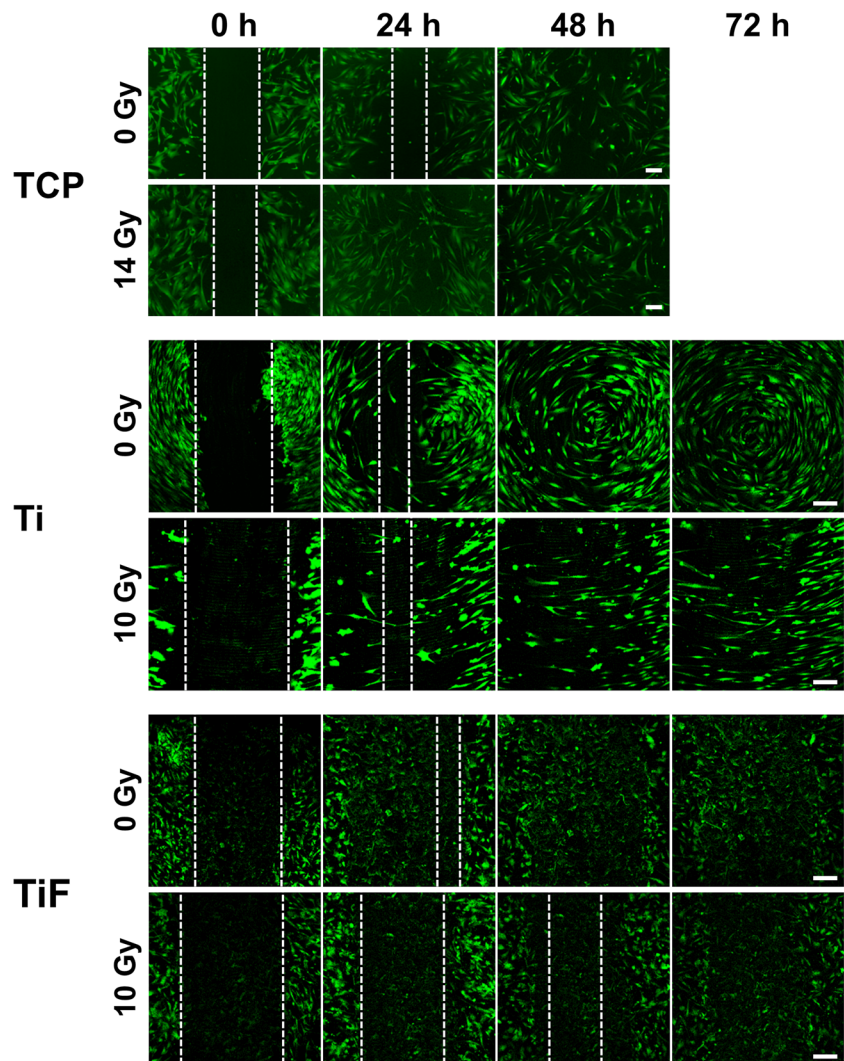
In contrast, *unirradiated* OBs and MSCs on TCP migrated the slowest and did not reach GC until 60 h after the initial scratch.

On the titanium surfaces (Ti and TiF), only the highest dose of 10 Gy slowed down the migration rate of both OBs (Figs. 2 and 3) and MSCs (Figs. 4 and 5).

Discussion

The comet assay is widely used for measuring DNA damage and repair in cells and tissues [32, 33], and the method has previously confirmed a linear relation between increased doses of ionizing irradiation and larger amounts of DNA damage in the exposed cells or organisms [29, 34, 35]. Correspondingly, this study showed increased DNA damage with increasing doses, but additional damage caused by radiation backscatter was only observed in the MSCs, especially from those irradiated on the minimally rough Ti-surface. In

general, the MSCs were significantly more affected than the OBs immediately after irradiation, irrespective of dose and surface. In fact, OBs irradiated on the TiF-surface showed no significantly increased DNA damage after any doses.

The substantially higher DNA damage found in MSCs after irradiation on the Ti-surface could explain why none of these disks retained a confluent monolayer of MSCs 24 h post-irradiation. On the other hand, MSCs were sustained on the TiF-surface after all irradiation doses, even though this surface induced the highest DNA damage in *unirradiated* MSCs, equaling the total damage in MSCs on the two titanium surfaces (Fig. S2, Online Resource). Hence, the absence of irradiated MSCs on the Ti disks could perhaps be linked to inhibition of adhesion rather than severe DNA damage.

Several studies have shown increased cell adhesion to rougher titanium surfaces compared to smooth or polished titanium [36–38], but also microscale and nanoscale modifications of the titanium such as biomimetic physicochemical
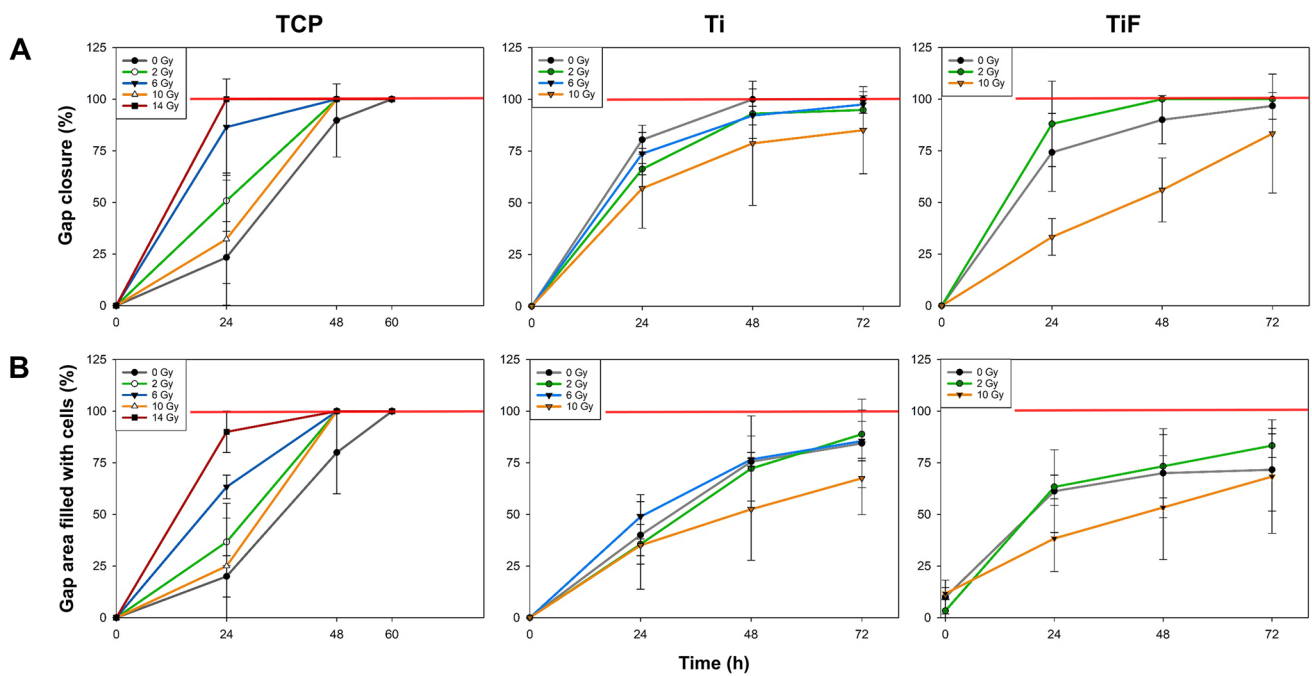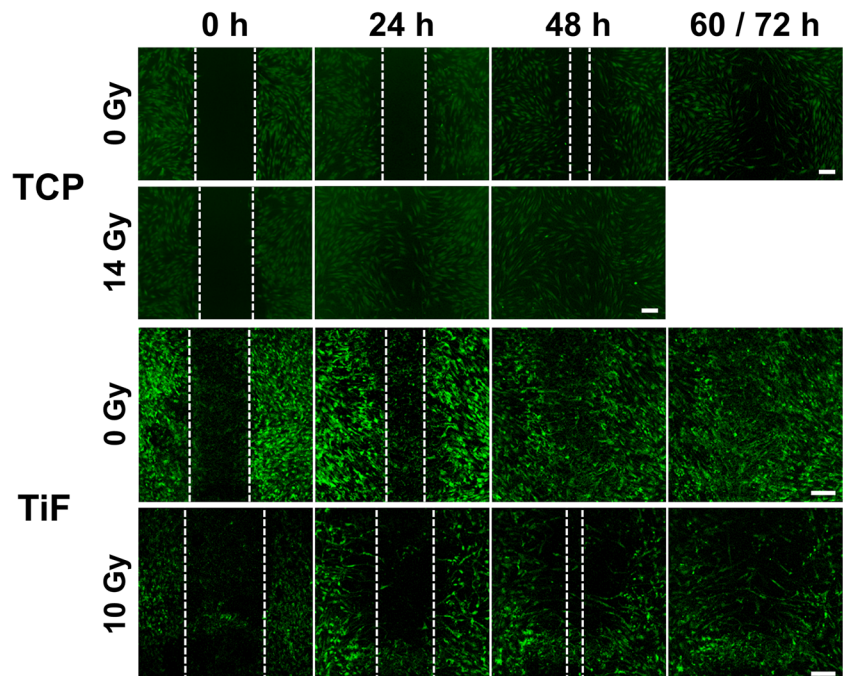
Fig. 3 Graphical illustration of the quantified **A** gap closure (GC) and **B** gap-area evenly filled with cells (GFC) on tissue culture polystyrene (TCP) after irradiation with 0, 2, 6, 10, and 14 Gy ($n=3$), on minimally rough machined titanium (Ti) after irradiation with 0 ($n=3$), 2 ($n=3$), 6 ($n=3$), and 10 ($n=2$) Gy, and on moderately rough fluoride-modified titanium (TiF) after irradiation with 0 ($n=4$), 2 ($n=3$), and 10 ($n=3$) Gy. Scratches were performed 24 h post-irradiation and images were captured at the timepoints 0, 24, 48, and 60 h (TCP) or 72 h (Ti and TiF) after the scratch. Data represent mean values $\pm$ SD

Fig. 4 Representative images of human mesenchymal stem cells (MSCs) migration and gap closure (GC) on tissue culture polystyrene (TCP) and moderately rough fluoride-modified titanium (TiF), after no irradiation and 14 Gy (TCP) or 10 Gy (TiF), at the timepoints 0, 24, 48, and 60 h (TCP) or 72 h (TiF). As full gap closure was already observed at 48 h for the 14 Gy TCP samples, no imaging was performed at 60 h. Scale bar: 200 μm

methods using proteins, peptides, and bioactive ceramics have shown to affect cell adhesion, spreading, and proliferation due to enhanced wettability of the surface [39, 40]. Accordingly, Li et al. found that irradiated osteoblast-like cells adhered stronger to a microarc oxidated titanium compared to a polished titanium, and surprisingly, also stronger than unirradiated controls [41]. However, another research group found that 5 and 10 days after irradiation,

Fig. 5 Graphical illustration of the quantified **A** gap closure (GC) and **B** gap-area evenly filled with cells (GFC) on tissue culture polystyrene (TCP) after irradiation with 0, 2, 6, 10, and 14 Gy ($n=3$), and on moderately rough fluoride-modified titanium (TiF) after irradiation with 0 ($n=3$), 2 ($n=3$), 6 ($n=4$), and 10 ($n=5$) Gy. Scratches were performed 24 h after irradiation and images were captured at the timepoints 0, 24, 48, and 60 h (TCP) or 72 h (Ti and TiF) after the scratch. Data represent mean values ± SD
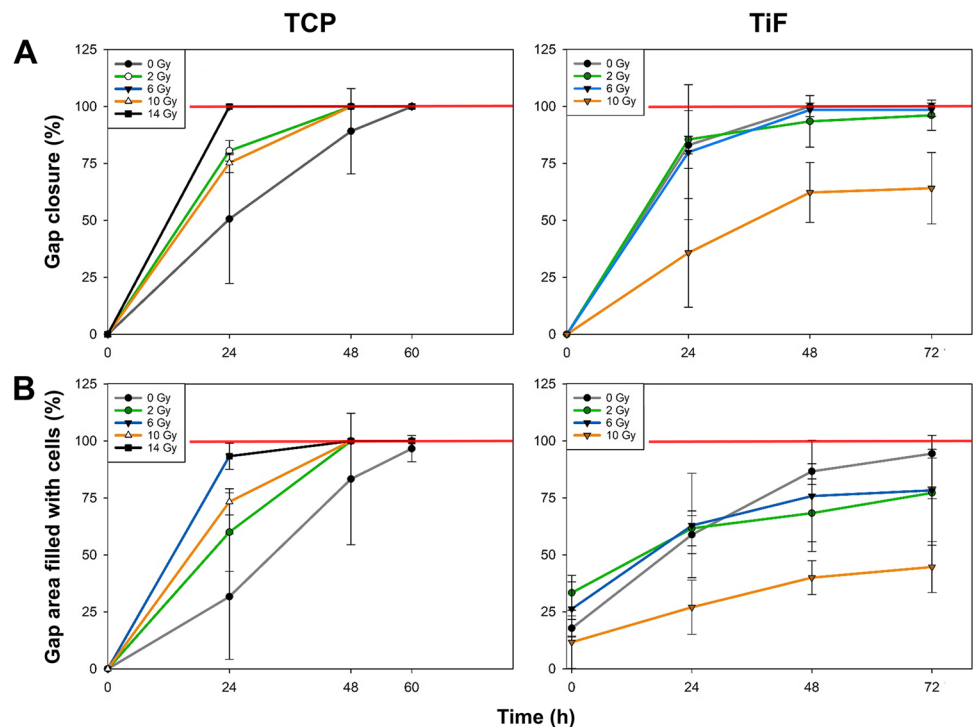
OBs attachment to both titanium and plastic decreased significantly [42]. In the present study, we experienced that both OBs and MSCs were difficult to remove from the TiF-surface with a pipette-tip, while on the Ti-surface, the entire cell sheet loosened in conjunction with the scratch in a pilot experiment. This may be explained by the higher surface roughness as well as higher wettability of the TiF surface compared to the Ti surface used in this study [43].

Based on a limited number of previous studies, OBs exposed to ionizing irradiation while cultured on titanium show a dose-dependent decrease in cell proliferation [41, 42, 44], while MSCs are known to be relatively radioresistant [28, 45]. Irradiation activates cell cycle checkpoints and DNA damage responses, but as revealed using the comet assay, early passage (2–3) MSCs are more resistant to irradiation and DNA damages induced by genotoxic agents than late-passage (> 10) MSCs [46]. Based on the knowledge that MSCs are quite radio-resistant, combined with the high DNA damage found immediately after irradiation, it seems like MSCs must inhere effective DNA repair mechanisms. Calini et al. showed that most DNA damage in mouse embryo fibroblasts exposed to high doses of irradiation (5 and 10 Gy) was repaired within 2 h, and the highest rejoining rate occurred with the highest dose of 10 Gy. Conversely, after a low dose of 1 Gy, no repair occurred within the first 2 h, but complete recovery was observed in all radiation groups after 24 h [34]. Another research group investigated the effects of γ-irradiation from a ^{60}Co source with doses ranging from 1 to 50 Gy, on a large number of *A.*

aegypti adult mosquitos. All radiation doses, except 1 Gy, exhibited a significant increase in DNA damage, with the highest levels observed 1 h post-irradiation. Total repair of damage occurred after 3 h in the 5 Gy group, after 6 h in the 10 Gy group, and after 12 h, no residual damage was found even in the 50 Gy group, although by then, heavily damaged cells may have been lost due to apoptosis [35]. Accordingly, we chose to initiate the scratch wound healing assay 24 h post-irradiation to ensure that all potential reversible DNA damage was repaired.

Even though the scratch assay is a simple, cost-effective, and very useful method to study cell migration in vitro [47], there are just a handful of such studies performed with cells growing on titanium [48, 49], and none of these is performed with cells exposed to ionizing irradiation. In this study, the migration capacity of OBs or MSCs growing on titanium was not altered by irradiation doses of 2 or 6 Gy, while a 10-Gy dose inhibited the migration, especially on the TiF-surface. The opposite was observed for both cell types on TCP, with increased migration after higher doses of irradiation. Although low-level laser irradiation and far-infrared irradiation have previously been shown to accelerate the migration of human OBs and rat bone marrow derived stem cells [50, 51], the considerably faster migration rate with full gap closure observed already after 24 h for both OBs and MSCs irradiated with a 14 Gy dose compared to 60 h for unirradiated cells on TCP was an unexpected finding. However, the results from the scratch assay support the assumption that most DNA damage observed in the cells

immediately after irradiation was repaired before initiating the assay 24 h post-irradiation, except after 10 Gy when reinforced with backscatter from titanium. Based on theoretical calculations, backscatter from titanium increases the relative effective radiation dose by more than 40% 10–20 μm from the implant surface, resulting in a 10-Gy dose on Ti and TiF corresponding to 14 Gy on TCP [28]. However, the backscattered radiation also has lower energy, and therefore, higher linear energy transfer (LET) than the primary radiation from the ^{60}Co source [52]. Higher LET is typically related to higher relative biological effectiveness of the radiation [53], which may explain both the increased DNA damage and the reduced migratory capacity of cells on the titanium surfaces compared to TCP exposed to theoretically corresponding radiation doses.

One limitation worth mentioning for the scratch assay is that proliferation needs to be inhibited to detect true cell migration. Avoiding serum in the cell culture medium is one way used to suppress cell proliferation [54]. Nonetheless, primary human cells need serum for the movement and overall survival, and therefore, totally serum-free medium is not recommended [30, 55]. Hence, using low serum concentrations as we did may inhibit, but not totally stop, cell proliferation. However, the clinical relevance of this study is not diminished even if the results may represent a combination of migration and proliferation, as ionizing irradiation also induces cell cycle delay and reduces cell proliferation [56].

Nevertheless, this is the first study to report in vitro migration of OBs and MSCs on a titanium implant surface after being exposed to ionizing irradiation with backscatter from titanium. The objective was to evaluate the effects of radiation backscatter on DNA damage and migration capacity of OBs and MSCs exposed to ionizing irradiation while growing on titanium. In conclusion, we found that radiation backscatter caused negative effects in form of increased DNA damage in MSCs immediately after irradiation, and reduced migration capacity of both OBs and MSCs after high doses of ionizing irradiation. However, low doses, as received in fractionated radiotherapy, do not seem to affect the migration of OBs or MSCs even when a dental titanium implant is generating radiation backscatter.

Author contribution L.P. was the project administrator and J.E.R., N.F.J.E., J.E.E, and H.T. acted as supervisors. L.P. and H.T. conceptualized and designed the study. L.P., H.T., J.E.R., and N.F.J.E. were responsible for the methodology. L.P. and H.T. curated and analyzed the data. L.P. and H.T. prepared the figures. L.P. and H.T. wrote the main manuscript text. J.E.E, J.E.R., and N.F.J.E. were responsible for resources and J.E.E. for funding acquisitions. All authors validated the study, reviewed, and approved the final manuscript as submitted.

Data Availability Data available on request from the authors.

Declarations

Ethics approval and consent to participate Not applicable.

Conflict of interest One of the authors, J. E. Ellingsen, has a patent licensing agreement with Dentsply Sirona Implants. The other authors declare no conflict of interest.

References

1. Jham BC, da Silva Freire AR (2006) Oral complications of radiotherapy in the head and neck. Braz J Otorhinolaryngol 72(5):704–708. https://doi.org/10.1016/s1808-8694(15)31029-6

2. Moore C, McLister C, O'Neill C, Donnelly M, McKenna G (2020) Pre-radiotherapy dental extractions in patients with head and neck cancer: a Delphi study. J Dent 97:103350. https://doi.org/10.1016/j.jdent.2020.103350

3. Beech N, Porceddu S, Batstone MD (2016) Preradiotherapy dental extractions and health-related quality of life. Oral Surg Oral Med Oral Pathol Oral Radiol 122(6):672–679. https://doi.org/10.1016/j.oooo.2016.07.020

4. Parahoo RS, Semple CJ, Killough S, McCaughan E (2019) The experience among patients with multiple dental loss as a consequence of treatment for head and neck cancer: a qualitative study. J Dent 82:30–37. https://doi.org/10.1016/j.jdent.2019.01.010

5. Brahm CO, Borg C, Malm D, Fridlund B, Lewin F, Zemar A, Nilsson P, Papias A, Henricson M (2021) Patients with head and neck cancer treated with radiotherapy: their experiences after 6 months of prophylactic tooth extractions and temporary removable dentures. Clin Exp Dent Res 7(5):894–902. https://doi.org/10.1002/cre2.418

6. Mijiritsky E, Ormianer Z, Klinger A, Mardinger O (2005) Use of dental implants to improve unfavorable removable partial denture design. Compend Contin Educ Dent 26(10):744–746, 748, 750 passim. https://www.ncbi.nlm.nih.gov/pubmed/16231543.

7. Kutkut A, Bertoli E, Frazer R, Pinto-Sinai G, Fuentealba Hidalgo R, Studts J (2018) A systematic review of studies comparing conventional complete denture and implant retained overdenture. J

Prosthodont Res 62(1):1–9. https://doi.org/10.1016/j.jpor.2017.06.004

8. Oh WS, Roumanas E, Beumer J 3rd (2007) Maxillofacial restoration after head and neck tumor therapy. Compend Contin Educ Dent 28(2):70–76; quiz 77, 101.

9. Vissink A, Spijkervet F, Raghoebar GM (2018) The medically compromised patient: are dental implants a feasible option? Oral Dis 24(1–2):253–260. https://doi.org/10.1111/odi.12762

10. Petrovic I, Rosen EB, Matros E, Huryn JM, Shah JP (2018) Oral rehabilitation of the cancer patient: a formidable challenge. J Surg Oncol 117(8):1729–1735. https://doi.org/10.1002/jso.25075

11. Petrovic I, Ahmed ZU, Matros E, Huryn JM, Shah JP, Rosen EB (2019) Endosseous (dental) implants in an oncologic population: a primer for treatment considerations. Quintessence Int 50(1):40–48. https://doi.org/10.3290/j.qi.a41336

12. Petrosyan V, Ball D, Harrison R, Ameerally P (2016) Among patients undergoing ablative treatment for oral cancer, does the provision of oral rehabilitation improve the quality of life? A review of the current literature. J Oral Maxillofac Surg 74(5):1096.e1091-1096.e1012. https://doi.org/10.1016/j.joms.2015.12.012

13. Woods B, Schenberg M, Chandu A (2019) A comparison of immediate and delayed dental implant placement in head and neck surgery patients. J Oral Maxillofac Surg 77(6):1156–1164. https://doi.org/10.1016/j.joms.2019.02.007

14. Alberga JM, Korfage A, Bonnema I, Witjes MJH, Vissink A, Raghoebar GM (2020) Mandibular dental implant placement immediately after teeth removal in head and neck cancer patients. Support Care Cancer 28(12):5911–5918. https://doi.org/10.1007/s00520-020-05431-y

15. Di Carlo S, De Angelis F, Ciolfi A, Quarato A, Piccoli L, Pompa G, Brauner E (2019) Timing for implant placement in patients treated with radiotherapy of head and neck. Clin Ter 170(5):e345–e351. https://doi.org/10.7417/ct.2019.2153

16. In't Veld M, Schulten E, Leusink FKJ (2021) Immediate dental implant placement and restoration in the edentulous mandible in head and neck cancer patients: a systematic review and meta-analysis. Curr Opin Otolaryngol Head Neck Surg 29(2):126–137. https://doi.org/10.1097/MOO.0000000000000685

17. Binger T, Seifert H, Blass G, Bormann KH, Rucker M (2008) Dose inhomogeneities on surfaces of different dental implants during irradiation with high-energy photons. Dentomaxillofac Radiol 37(3):149–153. https://doi.org/10.1259/dmfr/29131739

18. Sakamoto Y, Koike N, Takei H, Ohno M, Miwa T, Yoshida K, Shigematsu N, Kishi K (2017) Influence of backscatter radiation on cranial reconstruction implants. Br J Radiol 90(1070):20150537. https://doi.org/10.1259/bjr.20150537

19. Willers H, Held KD (2006) Introduction to clinical radiation biology. Hematol Oncol Clin North Am 20(1):1–24. https://doi.org/10.1016/j.hoc.2006.01.007

20. Peterson CL, Cote J (2004) Cellular machineries for chromosomal DNA repair. Genes Dev 18(6):602–616. https://doi.org/10.1101/gad.1182704

21. Wang X, Li B (2007) Genetic studies of bone diseases: evidence for involvement of DNA damage response proteins in bone remodeling. Int J Biomed Sci 3(4):217–228. https://www.ncbi.nlm.nih.gov/pubmed/23675047

22. Zhou BB, Elledge SJ (2000) The DNA damage response: putting checkpoints in perspective. Nature 408(6811):433–439. https://doi.org/10.1038/35044005

23. Willers H, Heilmann HP, Beck-Bornholdt HP (1998) One hundred years of radiotherapy. Historical origins and development of fractionated irradiation in German speaking countries. Strahlenther Onkol 174(2):53–63. https://doi.org/10.1007/bf03038475

24. Raghavendra S, Wood MC, Taylor TD (2005) Early wound healing around endosseous implants: a review of the literature. Int J Oral Maxillofac Implants 20(3):425–431

25. Terheyden H, Lang NP, Bierbaum S, Stadlinger B (2012) Osseointegration–communication of cells. Clin Oral Implants Res 23(10):1127–1135. https://doi.org/10.1111/j.1600-0501.2011.02327.x

26. Suzuki R, Takakuda K (2016) Wound healing efficacy of a 660-nm diode laser in a rat incisional wound model. Lasers Med Sci 31(8):1683–1689. https://doi.org/10.1007/s10103-016-2038-0

27. Wang YH, Wu JY, Kong SC, Chiang MH, Ho ML, Yeh ML, Chen CH (2018) Low power laser irradiation and human adipose-derived stem cell treatments promote bone regeneration in critical-sized calvarial defects in rats. PLoS One 13(4):e0195337. https://doi.org/10.1371/journal.pone.0195337

28. Printzell L, Reseland JE, Edin NFJ, Ellingsen JE (2019) Effects of ionizing irradiation and interface backscatter on human mesenchymal stem cells cultured on titanium surfaces. Eur J Oral Sci 127(6):500–507. https://doi.org/10.1111/eos.12654

29. Kumaravel TS, Jha AN (2006) Reliable Comet assay measurements for detecting DNA damage induced by ionising radiation and chemicals. Mutat Res 605(1–2):7–16. https://doi.org/10.1016/j.mrgentox.2006.03.002

30. Liang CC, Park AY, Guan JL (2007) In vitro scratch assay: a convenient and inexpensive method for analysis of cell migration in vitro. Nat Protoc 2(2):329–333. https://doi.org/10.1038/nprot.2007.30

31. Schneider CA, Rasband WS, Eliceiri KW (2012) NIH Image to ImageJ: 25 years of image analysis. Nat Methods 9(7):671–675. https://doi.org/10.1038/nmeth.2089

32. Møller P (2018) The comet assay: ready for 30 more years. Mutagenesis 33(1):1–7. https://doi.org/10.1093/mutage/gex046

33. Liao W, McNutt MA, Zhu W-G (2009) The comet assay: a sensitive method for detecting DNA damage in individual cells. Methods 48(1):46–53. https://doi.org/10.1016/j.ymeth.2009.02.016

34. Calini V, Urani C, Camatini M (2002) Comet assay evaluation of DNA single- and double-strand breaks induction and repair in C3H10T1/2 cells. Cell Biol Toxicol 18(6):369–379. https://doi.org/10.1023/a:1020811522100

35. Shetty V, Shetty NJ, Ananthanarayana SR, Jha SK, Chaubey RC (2017) Evaluation of gamma radiation-induced DNA damage in Aedes aegypti using the comet assay. Toxicol Ind Health 33(12):930–937. https://doi.org/10.1177/0748233717733599

36. Zhu X, Chen J, Scheideler L, Altebaeumer T, Geis-Gerstorfer J, Kern D (2004) Cellular reactions of osteoblasts to micron- and submicron-scale porous structures of titanium surfaces. Cells Tissues Organs 178(1):13–22. https://doi.org/10.1159/000081089

37. Zhu X, Chen J, Scheideler L, Reichl R, Geis-Gerstorfer J (2004) Effects of topography and composition of titanium surface oxides on osteoblast responses. Biomaterials 25(18):4087–4103. https://doi.org/10.1016/j.biomaterials.2003.11.011

38. Zhao L, Wei Y, Li J, Han Y, Ye R, Zhang Y (2010) Initial osteoblast functions on Ti-5Zr-3Sn-5Mo-15Nb titanium alloy surfaces modified by microarc oxidation. J Biomed Mater Res A 92(2):432–440. https://doi.org/10.1002/jbm.a.32348

39. Souza JCM, Sordi MB, Kanazawa M, Ravindran S, Henriques B, Silva FS, Aparicio C, Cooper LF (2019) Nano-scale modification of titanium implant surfaces to enhance osseointegration. Acta Biomater 94:112–131. https://www.sciencedirect.com/science/article/pii/S1742706119303721?via%3Dihub

40. Parisi L, Ghezzi B, Bianchi MG, Toffoli A, Rossi F, Bussolati O, Macaluso GM (2020) Titanium dental implants hydrophilicity promotes preferential serum fibronectin over albumin competitive adsorption modulating early cell response. Mater Sci Eng C Mater

Biol Appl 117:111307. https://www.sciencedirect.com/science/article/pii/S0928493120332252?via%3Dihub

41. Li Y, Ma W, Feng Z, Wang Z, Zha N, Deng B, Zhao Y (2013) Effects of irradiation on osteoblast-like cells on different titanium surfaces in vitro. J Biomed Mater Res B Appl Biomater 101(1):9–17. https://doi.org/10.1002/jbm.b.32803

42. Ahmad M, Sampair C, Nazmul-Hossain AN, Khurana N, Nerness A, Wutticharoenmongkol P (2008) Therapeutic doses of radiation alter proliferation and attachment of osteoblasts to implant surfaces. J Biomed Mater Res A 86(4):926–934. https://doi.org/10.1002/jbm.a.31737

43. Printzell L, Reseland JE, Edin NFJ, Tiainen H, Ellingsen JE (2023) The dose-dependent impact of γ-radiation reinforced with backscatter from titanium on primary human osteoblasts, Biomater Investig Dent 10(1):2209116. https://www.tandfonline.com/doi/pdf/10.1080/26415275.2023.2209116

44. Dare A, Hachisu R, Yamaguchi A, Yokose S, Yoshiki S, Okano T (1997) Effects of ionizing radiation on proliferation and differentiation of osteoblast-like cells. J Dent Res 76(2):658–664. https://doi.org/10.1177/00220345970760020601

45. Nicolay NH, Liang Y, Lopez Perez R, Bostel T, Trinh T, Sisombath S, Weber KJ, Ho AD, Debus J, Saffrich R, Huber PE (2015) Mesenchymal stem cells are resistant to carbon ion radiotherapy. Oncotarget 6(4):2076–2087. https://doi.org/10.18632/oncotarget.2857

46. Wu PK, Wang JY, Chen CF, Chao KY, Chang MC, Chen WM, Hung SC (2017) Early passage mesenchymal stem cells display decreased radiosensitivity and increased DNA repair activity. Stem Cells Transl Med 6(6):1504–1514. https://doi.org/10.1002/sctm.15-0394

47. Grada A, Otero-Vinas M, Prieto-Castrillo F, Obagi Z, Falanga V (2017) Research techniques made simple: analysis of collective cell migration using the wound healing assay. J Invest Dermatol 137(2):e11–e16. https://doi.org/10.1016/j.jid.2016.11.020

48. Zhukova Y, Hiepen C, Knaus P, Osterland M, Prohaska S, Dunlop JWC, Fratzl P, Skorb EV (2017) The role of titanium surface nanostructuring on preosteoblast morphology, adhesion, and migration. Adv Healthc Mater 6(15). https://doi.org/10.1002/adhm.201601244.

49. Amberg R, Elad A, Rothamel D, Fienitz T, Szakacs G, Heilmann S, Witte F (2018) Design of a migration assay for human gingival fibroblasts on biodegradable magnesium surfaces. Acta Biomater 79:158–167. https://doi.org/10.1016/j.actbio.2018.08.034

50. Tsuka Y, Kunimatsu R, Gunji H, Nakajima K, Kimura A, Hiraki T, Nakatani A, Tanimoto K (2019) Effects of Nd:YAG low-level laser irradiation on cultured human osteoblasts migration and ATP production: in vitro study. Lasers Med Sci 34(1):55–60. https://doi.org/10.1007/s10103-018-2586-6

51. Jeong YM, Cheng XW, Lee S, Lee KH, Cho H, Kang JH, Kim W (2017) Preconditioning with far-infrared irradiation enhances proliferation, cell survival, and migration of rat bone marrow-derived stem cells via CXCR4-ERK pathways. Sci Rep 7(1):13718. https://doi.org/10.1038/s41598-017-14219-w

52. Pibida L, West D (2018) Measurements of scatter peaks in (137) Cs and (60)Co sources. J Res Natl Inst Stand Technol 123:1–16. https://doi.org/10.6028/jres.123.012

53. Mladenova V, Mladenov E, Iliakis G (2016) Novel biological approaches for testing the contributions of single DSBs and DSB clusters to the biological effects of high LET radiation. Front Oncol 6:163. https://doi.org/10.3389/fonc.2016.00163

54. Martinotti S, Ranzato E (2020) Scratch wound healing assay. Methods Mol Biol 2109:225–229. https://doi.org/10.1007/7651_2019_259

55. Vang Mouritzen M, Jenssen H (2018) Optimized scratch assay for in vitro testing of cell migration with an automated optical camera. J Vis Exp (138). https://doi.org/10.3791/57691.

56. Lau P, Baumstark-Khan C, Hellweg CE, Reitz G (2010) X-irradiation-induced cell cycle delay and DNA double-strand breaks in the murine osteoblastic cell line OCT-1. Radiat Environ Biophys 49(2):271–280. https://doi.org/10.1007/s00411-010-0272-6